

2) A “dwarf planet” is a celestial body that...

- a) is in orbit around the Sun,
- b) has sufficient mass for its self-gravity **to overcome rigid body forces** so that it assumes a hydrostatic equilibrium (nearly round) shape²,
- c) has not cleared the neighbourhood around its orbit, and
- d) is not a satellite.

Ref. IAU Res. GA 26 B5

Ceres, Pluto, Eris, Makemake, Haumea, ...

Sphericity

- $\psi = \pi^{1/3}(6V)^{2/3}/S \leq 1$,
i.e. volume vs surface
(Wadell 1935)
- asphericity $1 - \psi$
- 3D shape model...
- multipole expansion
(10th order)
- ψ of Hygiea ~ Ceres
- both C-types

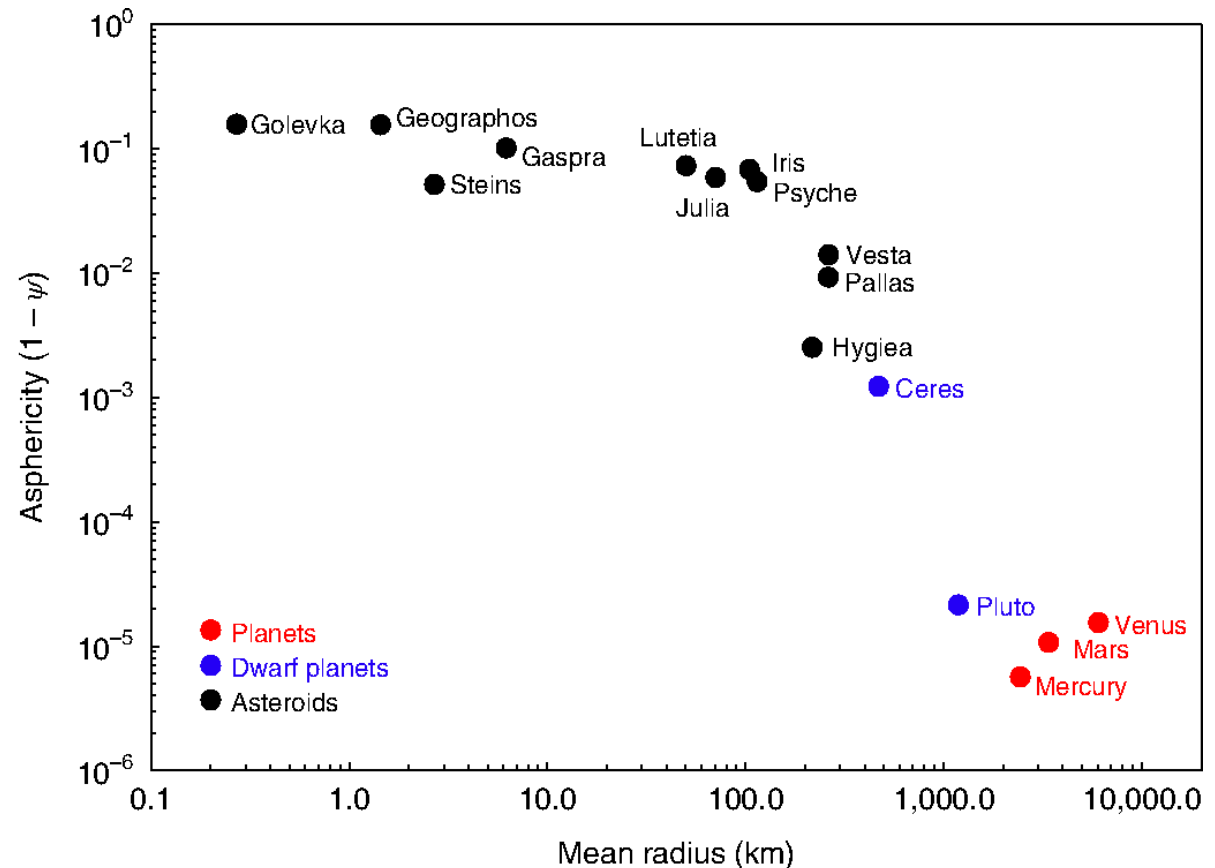
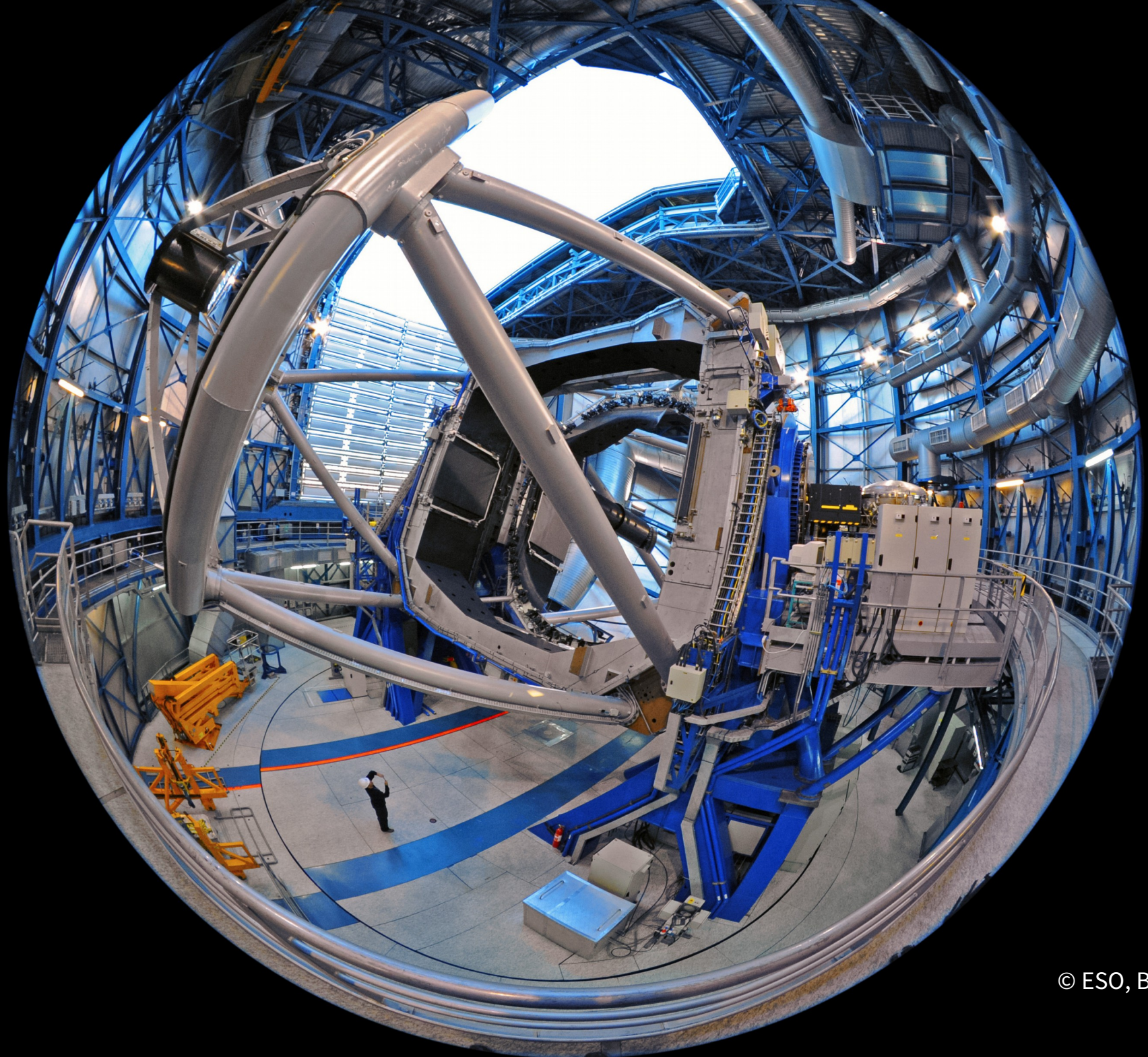


Fig. 4 | Asphericity of Solar System objects as a function of their mean radius. The parameter ψ corresponds to the sphericity index²⁶ applied to spherical harmonics developments of the 3D shape models of each object. Hygiea appears nearly as spherical as the dwarf planet Ceres.

Reviews

- description SPH w. self-gravity? ← see Ševeček et al. (2019)
- use **friction!** ← but Hygiea is round
- 4-h timescale of fluidisation? ← another t. *not* applicable
- $c_s = 3 \text{ km s}^{-1}$, crossing time $t = D/c_s = 170 \text{ s}$, i.e. $\sim 10^2$ crossings
- **self-gravity** must overcome rigid-body forces (not r.)
- cratering (cf. Carruba et al. 2014)? ← SFD is reaccumulated
c. → reaccumulative → catastrophic → super-catastrophic
- age 1.3 Gy (cf. Spoto et al. 2015)? ← $v_{\text{esc}} = 226 \text{ m/s}$, $v_{\text{ej}} \sim v_{\text{esc}}$



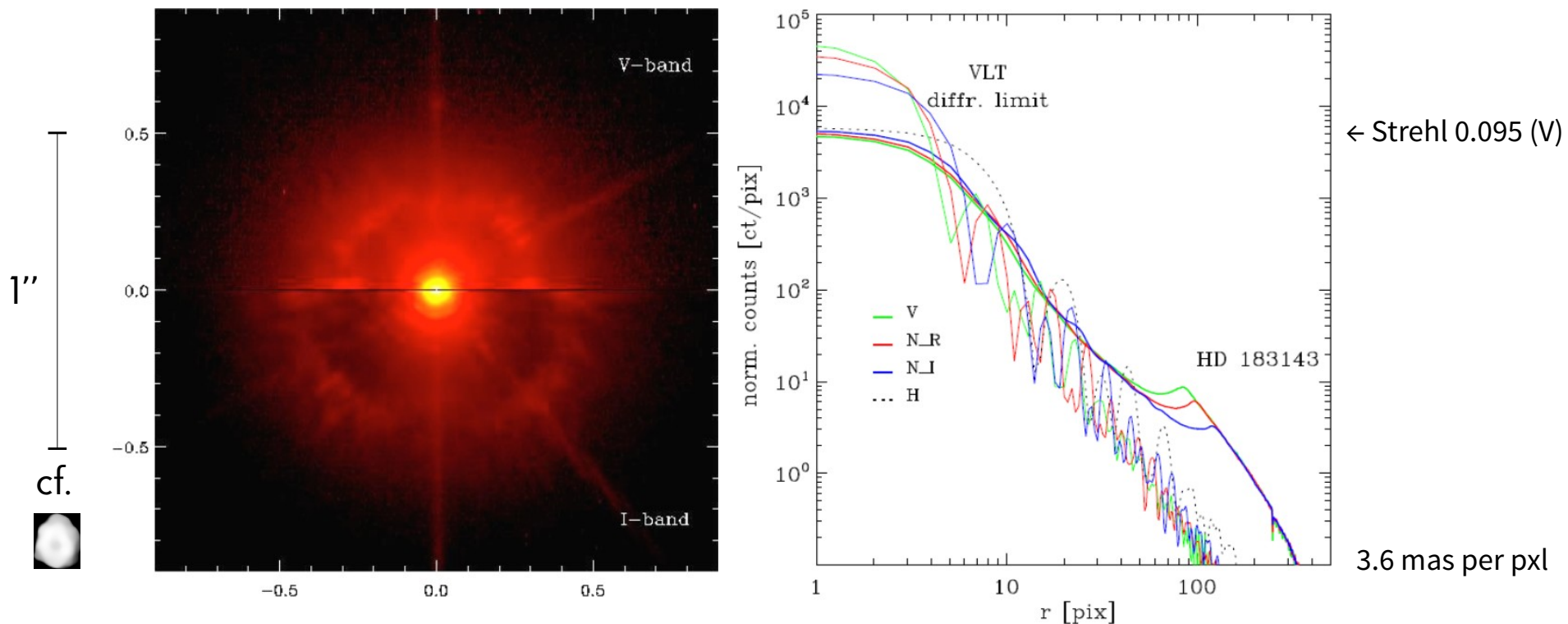
AO imaging \neq direct i.

- stellar vs semi-analytic, axisymmetric (Moffat) **PSF**
- deconvolution algorithms w. priors, regularisation
- non-convex shape model (ADAM; Viikinkoski *etal.* 2015),
- or **inclinometry** (Jorda *etal.* *in prep.*)
- limited phase coverage vs “geological mapping”



PSF & its variability

- N_R filter (645 ± 28 nm), dependence on λ , seeing ($<0.8''$)
- asteroid as NGS, nearby * as PSF, 5 of 10-s exposures @ epoch



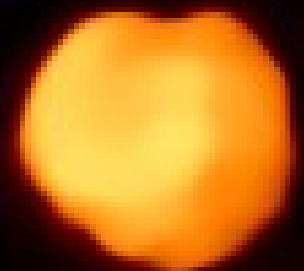
degraded image



stellar PSF



deconvolved image



=

*

Deconvolution (Bayes statistics)

- I ... degraded image, H ... PSF, O ... ideal image, N ... Noise

$$I = H * O + N$$

- Bayes theorem for conditional probabilities, where $p(I) = I \div 65535$ ADU

$$p(O \wedge I) = p(O|I)p(I) = p(I|O)p(O) \rightarrow p(O|I) = \frac{p(I|O)p(O)}{p(I)}$$

- maximalisation of $p(O|I)$, i.e. minimalisation of the functional wrt. O :

$$J = -\ln[p(I|O)p(O)] = -\ln p(I|O) - \ln p(O) \equiv J_N + J_O$$

Myopic deconvolution ← MISTRAL algorithm

- problems of Richardson-Lucy: **divergence** (if not Poisson), artifacts, “ringing”
- Gaussian noise (photon, PSF, seeing, jitter, ...), regularisation (Conan et al. 2000):

$$p(x; \sigma) = \frac{1}{\sigma\sqrt{2\pi}} e^{-\frac{x^2}{2\sigma^2}} \quad \rightarrow \quad J_N = \sum_r \frac{1}{2\sigma^2} (I - H * O)^2$$

- additional priors (edge, seeing), 2nd regularisation:

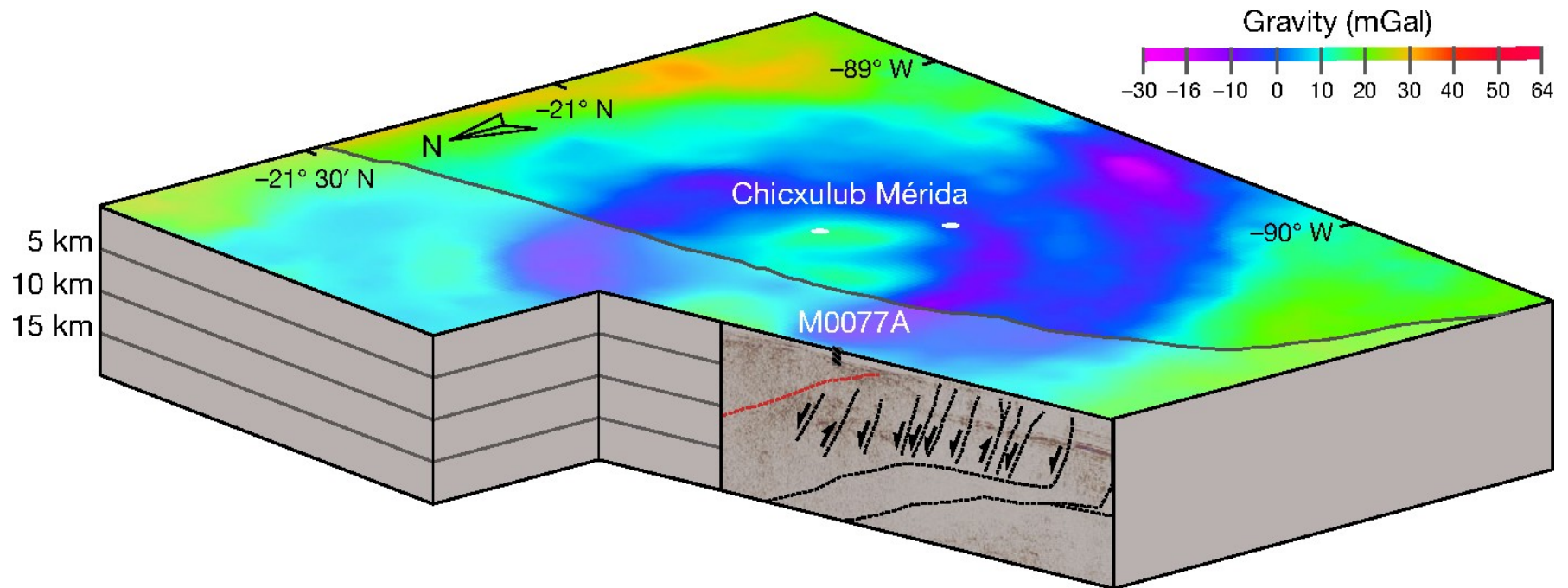
$$J_O = -\ln p(O) = \mu \sum_r \left[\frac{|\nabla O|}{\delta} - \ln \left(1 + \frac{|\nabla O|}{\delta} \right) \right]$$

δ, μ ... free parameters,
 $E()$... expectation (average over λ),
 \tilde{H} ... Fourier transform, i.e. MTF

$$J_H = \frac{1}{2} \sum_q \frac{|\tilde{H} - E(\tilde{H})|^2}{E[|\tilde{H} - E(\tilde{H})|^2]}$$

Acoustic fluidisation ← experiment

- block model (Melosh 1989)
- used for Vesta (Jutzi et al. 2013), or **Chicxulub** (Riller et al. 2018)



also higher-order oscillations?

Riller et al. (2018); $c_s = 3 \text{ km/s}$, $D = 30 \text{ km}$, $t \sim 10^1 \text{ s}$, but ring & peak collapse \rightarrow more sound waves...

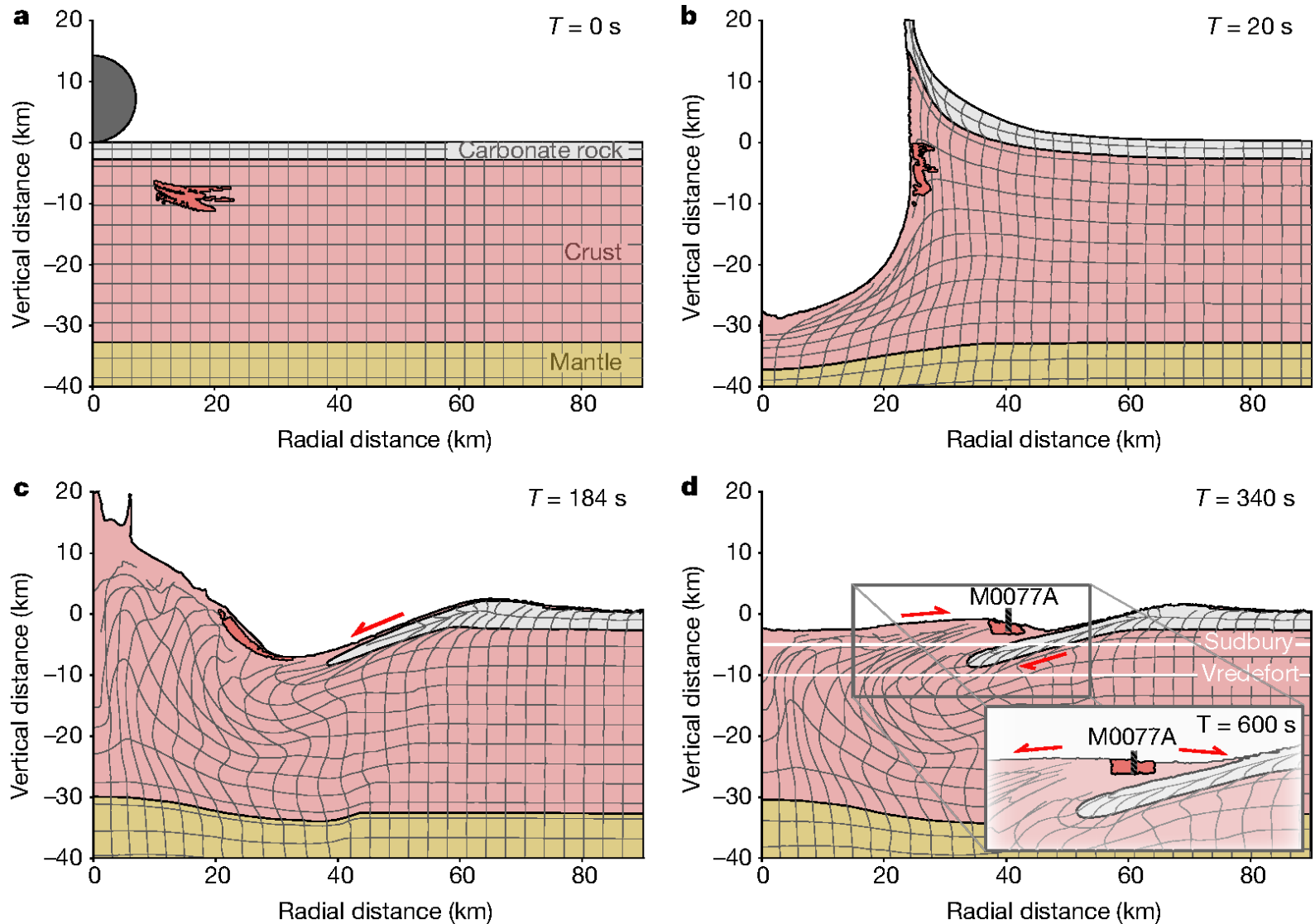


Fig. 2 | Modelled formation of the Chicxulub impact structure. The mechanism is based on numerical modelling of peak-ring crater formation^{4,23,24,34}. A grid of tracer particles is shown to highlight the sub-crater deformation. Dark red area of crust in each panel tracks the material that eventually forms the peak ring. T denotes time in seconds after impact. Red half-arrows indicate the direction of major shear displacements relative to adjacent material. **a**, Undisturbed configuration of model lithosphere before impact. **b**, Cratering starts by shock-wave-

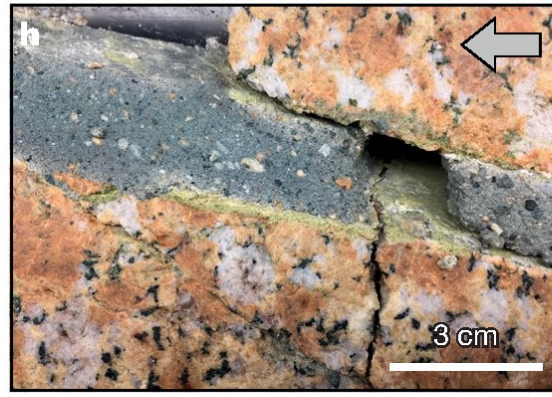
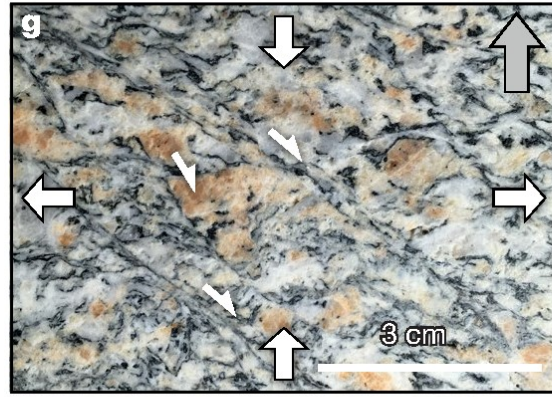
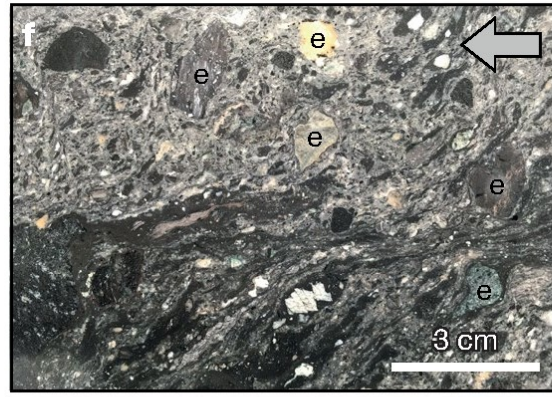
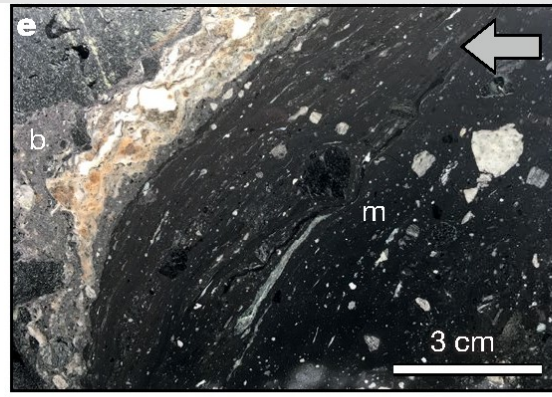
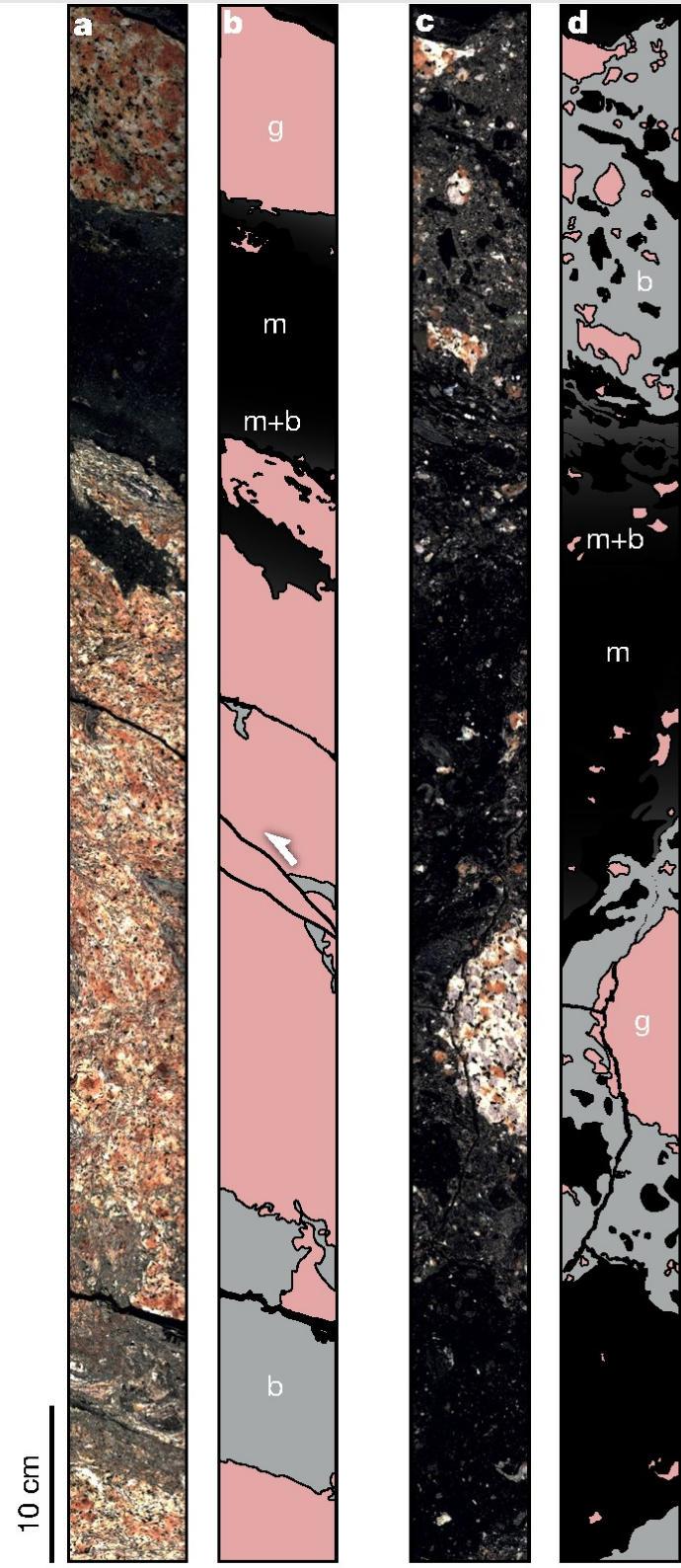
induced, crustal-scale excavation of a bowl-shaped transient cavity. **c**, Gravitational instability of the transient cavity causes uplift of the crater centre and concomitant inward slumping of the cavity wall. **d**, Collapse and radial outward displacement of uplifted material over inward-slumped cavity wall segments followed by gravitational settling of the peak ring (inset) characterize the terminal phase of modelled crater modification. White lines indicate the approximate current erosion levels of the Sudbury and Vredefort impact structures.

Riller et al. (2018)

g ... granitoid

m ... melt

b ... breccia



e ... „exotic“
shear zone

horizontal extension
vertical shortening

c ... cataclasite
fracture